Cell Biochem Biophys (2013) 66:657–669
DOI 10.1007/s12013-012-9510-7

ORIGINAL PAPER

Identification of Potential Inhibitors of H5N1 Influenza A Virus Neuraminidase by Ligand-Based Virtual Screening Approach

V. Karthick · K. Ramanathan · V. Shanthi · R. Rajasekaran

Published online: 10 January 2013

Abstract The neuraminidase (NA) of the influenza virus is the target of antiviral drug, oseltamivir. Recently, cases were reported that influenza virus becoming resistant to oseltamivir, necessitating the development of new long-acting antiviral compounds. In this report, a novel class of lead molecule with potential NA inhibitory activity was identified using a combination of virtual screening (VS), molecular docking, and molecular dynamic approach. The PubChem database was used to perform the VS analysis by employing oseltamivir as query. Subsequently, the data reduction was carried out by employing molecular docking study. Furthermore, the screened lead molecules were analyzed with respect to the Lipinski rule of five, drug-likeness, toxicity profiles, and other physico-chemical properties of drugs by suitable software program. Final screening was carried out by normal mode analysis and molecular dynamic simulation approach. The result indicates that CID 25145634, deuterium-enriched oseltamivir, become a promising lead compound and be effective in treating oseltamivir sensitive as well as resistant influenza virus strains.

Keywords Neuraminidase · Oseltamivir-resistance · Virtual screening · Molecular docking · Molecular dynamic simulation

V. Karthick · K. Ramanathan (✉) · R. Rajasekaran
Bioinformatics Division, School of Bio Sciences and Technology, Vellore Institute of Technology, Vellore 632014, Tamil Nadu, India
e-mail: kramanathan@vit.ac.in

V. Shanthi
Industrial Biotechnology Division, School of Bio Sciences and Technology, Vellore Institute of Technology, Vellore 632014, Tamil Nadu, India

Introduction

The pandemic influenza A (H5N1) virus has spread rapidly and raised global concern for the human health. It can be classified by the antigenic properties of two surface glycoproteins, hemagglutinin (HA) and neuraminidase (NA). Hemagglutinin has 16 subtypes (H1, H2, H3… H16) and NA (N1, N2, N3… N9) has nine subtypes [1, 2]. These glycoproteins (HA and NA) together play an important role in the interactions between the virus and the host cell surface receptors [3]. In humans, influenza viruses preferentially bind to sialic acid-α 2,6-galactose [4]. HA antigen binds to the sialic acid receptor on the cell surface, which mediates the virus entry. The NA cleaves the specific linkage of the sialic acid receptor, resulting in the release of the newly formed virions from the infected cells. Additionally, the NA may function to facilitate the early process of influenza virus infection of lung epithelial cells [3, 5, 6]. Because of its essential role in the release of the influenza virus particles, NA inhibition is a pivotal step in restricting the spread of influenza virus infection in the host.

Oseltamivir (Tamiflu) and zanamivir (Relenza) are two currently used NA inhibitors that were developed using the knowledge of the enzyme structure. However, they are completely different in terms of mode of delivery, pharmacological action, and side effects. Zanamivir has poor oral availability and is therefore administered by inhalation only and has limited usage when treating the elderly person because it may induce bronchospasm. Also there are reports of zanamivir resistance [7]. Oseltamivir is the preferred antiviral drug for influenza. Oseltamivir is an orally active influenza NA inhibitor approved for treating and preventing influenza virus infection. However, oseltamivir-resistant A (H5N1) viruses have circulated worldwide since the

2007–2008 influenza season [8]. Furthermore, there have been reports of oseltamivir-resistant mutant selection in vitro and from infected humans [9–12]. In particular, H274Y, the principal mutation isolated in association with oseltamivir treatment that is specific to the N1 group [13] and that has recently been shown to be present in substantial numbers of H5N1 viruses isolated from humans [14]. To accommodate the bulky side chain of oseltamivir in the active site, the NA molecule must undergo rearrangement to create a pocket. The H274Y mutation limits the necessary molecular rearrangement and may diminish the binding of oseltamivir [15]. The notion of high-affinity binding implies a longer residence time for the ligand at its binding site than in the case for low-affinity binding. So the decrease in binding affinity between the NA and the oseltamivir decrease its drug efficacy toward the NA [16]. This continuous threat of imminent pandemics [17, 18] and the emergence of resistant strains to oseltamivir prompt continuous research toward developing new and more effective NA inhibitors [11].

Virtual screening (VS) is a widely used method that has been shown to be successful in a variety of studies, although it also has many shortcomings [19, 20]. In the past few years, many reports indicated that VS techniques proved to be effective in making qualitative predictions that discriminated active from inactive compounds [21]. The use of experimentally derived protein structures and a hybrid computational method that combines the advantages of docking algorithms with dynamic structural information provided by normal mode analysis (NMA) has been successfully applied to a number of systems [22, 23] and most recently, aid in the discovery of novel compounds active against the p53 tumor repressor [24].

In this study, a combined molecular docking and molecular simulation approach have been applied to screen the potential molecule from PubChem database maintained by NCBI [25, 26] against the drug-resistant target of NA. PubChem is a public molecular information repository, a scientific showcase of the NIH Roadmap Initiative. The PubChem database holds over 27 million records of unique chemical structures of compounds (CID) derived from nearly 70 million substance depositions and contains more than 449,000 bioassay records with over thousands of in vitro biochemical and cell-based screening bioassays established, with targeting more than 7,000 proteins and genes linking to over 1.8 million of substances. These publicly available datasets in PubChem provide great opportunities for scientists to perform cheminformatics and VS research for computer-aided drug design [27]. Hence, in this study, we have used Pubchem database for our computational analysis. Hopefully, we have proposed some useful candidates for H5N1 and put forward a constructive concept of designing H5N1 inhibitors.

Materials and Methods

Data Set Preparation

The native- and mutant (H274Y)-type coordinates of NA were taken from the Brookhaven Protein Data Bank (PDB) [28]. The corresponding PDB codes were 2HTY and 3CL0, respectively. The structures were solved with 2.50 and 2.20 Å resolutions, respectively, having residues from 83 to 468. Oseltamivir was used as the small molecule/inhibitor for our investigation. The SMILES strings were collected from PubChem, a database maintained in NCBI [25, 26], and submitted to CORINA for constructing the 3D structure of the small molecule [29]. The three-dimensional structure of target proteins (2HTY and 3CL0) and drug molecule was energy-minimized using GROMACS package 4.5.3 [30, 31] adopting the GROMOS43a1 force field parameters before performing the computational analysis.

Virtual Screening

Virtual screening [32] is the computational analogue of biological screening. The approach has become increasingly popular in the pharmaceutical research for lead identification. The basic goal of the VS is the reduction of the massive virtual chemical space of small organic molecules, to screen against a specific target protein, to a manageable number of the compound that inhibit a highest chance to lead to a drug candidate [33]. The PubChem database was used for searching new lead compounds by employing the oseltamivir as query [25, 26]. The numbers of molecules in the database is around 85 million compounds. Several hits were obtained from the database, which were further screened using molecular docking studies.

Molecular Docking

The docking procedure first involved with specification of the ligand binding site in a receptor and then docking ligands into the specified site. The amino acids around the binding site were analyzed based on the information available from the literatures [34, 35]. The lead compounds obtained from the VS analysis were used in the docking calculation. The SMILES strings were used for constructing three-dimensional structures of all the lead compounds. After docking, the compounds were ranked based on the geometric matching score with target proteins. The geometric matching score of oseltamivir with target proteins (native and mutant structures) were used as reference for filtering the lead compounds. The energy-minimized structures of NA were used as a template molecule to dock known and unknown inhibitors. In this study, rigid docking analysis was performed by means of Patchdock program [36]. It is geometry-based molecular docking algorithm. The PatchDock algorithm divides the Connolly dot surface representation [37, 38] of the molecules into concave, convex, and flat patches. Then, complementary patches are matched to generate candidate transformations. Each candidate transformation is further evaluated by a scoring function that considers both geometric fit and atomic desolvation energy [39]. Finally, root mean square deviation (RMSD) clustering is applied to the candidate solutions to discard redundant solutions. The input parameters for the docking are the PDB coordinate file of the protein and ligand molecule. This algorithm has three major stages: (i) molecular shape representation, (ii) surface patch matching, and (iii) filtering and scoring.

ADME and Toxicity

Molecular properties such as membrane permeability and bioavailability are always associated with some basic molecular descriptors such as logP (partition coefficient), molecular weight (MW), or counts of hydrogen bond acceptors and donors in a molecule [40]. These molecular properties were used in formulating ''rule of five'' [41] The rule states that most molecules with good membrane permeability have MW $\leq$500, calculated octanol–water partition coefficient, log $P \leq 5$, hydrogen bond donors $\leq$5, acceptors $\leq$10, and van der Waals bumps polar surface area (PSA) <120 Å^2 [42]. Therefore, Lipinski's Rule of Five were used to test the bioavailability characteristics such as adsorption, distribution, metabolism, elimination (ADME) of the lead compounds. In this study, these molecular properties for all the lead compounds were estimated using MOLINSPIRATION program [43].

Additional screening was also carried out by restricting the number of rotatable bonds to a maximum of ten [44, 45]. Successful drug discovery requires high-quality lead structures which may need to be more drug-like than commonly accepted [46]. Toxicity and poor pharmacokinetics should be eliminated in the early stages of drug discovery. Hence, the hits were further screened using drug-likeliness, drug score, and toxicity characteristics. These physico-chemical properties were therefore calculated for the filtered set of hits using the programs OSIRIS [47].

The OSIRIS program calculates the drug-likeliness based on a list of about 5,300 distinct substructure fragments created by 3,300 traded drugs as well as 15,000 commercially available chemicals yielding a complete list of all available fragments with associated drug-likeliness. The drug score combines drug-likeliness, cLogP, logS, MW, and toxicity risks as a total value which may be used to judge the compound's overall potential to qualify for a drug.

Normal Mode Analysis

The exploration of molecular motions of biological molecules and their assemblies by simulation approaches such as molecular dynamics has provided significant insights into structure-function relationships in small biological systems. NMA provides an alternative to molecular dynamics for studying the motions of macromolecules. The time-scale accessible to theoretical work is extended with NMA, and this approach has been proven extremely useful for studying collective motions of biological systems. NMA is a powerful tool for predicting the possible movements of a given macromolecule. It has been shown recently that half of the known protein movements can be modeled using at most two low-frequency normal modes [48]. Applications of NMA cover wide areas of structural biology, such as the study of protein conformational changes upon ligand binding, membrane channel opening and closure, potential movements of the ribosome, and viral capsid maturation. Another, newly emerging field of NMA is related to protein structure determination by X-ray crystallography, where normal mode perturbed models are used as templates for diffraction data phasing through molecular replacement MR). ElNemo is a web interface to the Elastic Network Model that provides a fast and simple tool to compute, visualize and analyze low-frequency normal modes of large macro-molecules and to generate a large number of different starting models for use in molecular replacement [49, 50]. Using this interface, each docked complex was analyzed with default parameters to investigate the active site residues by NMA.

Molecular Dynamics Simulation

The docked complexes such as native type of NA–oseltamivir, mutant type of NA–oseltamivir, native type of NA–CID 25145634 and mutant-type of NA–CID 25145634 were used as starting point for MD simulation using GROMACS package 4.5.3 [30, 31] adopting the GROMOS43a1 force field parameters. The structures were solvated in cubic 0.9 nm, using periodic boundary conditions and the SPC water model [51]. PRODRG server [52] was used to generate ligand topology. 4Na$^+$ counter ions were added to neutralize the total charge of the system. 1,000 steps of steepest descent energy minimization were carried out for the protein–ligand complex. After energy minimization, the system was equilibrated at constant temperature and pressure. The equilibrated structures were then subjected to molecular dynamic simulations for 20,000 ps, and the integration time step was set to 2 fs. The non-bonded list was generated, using an atom-based cutoff of 8 Å. The long range electrostatic interactions were handled by the particle-mesh Ewald algorithm [53]. 0.9 nm cutoff was employed to Lennard–Jones interaction. During the simulations, all bond lengths containing hydrogen atoms were constrained utilizing the Lincs algorithm [54], the trajectory snapshots were stored for structural analysis at every pico-second. RMSD, radial distribution function and H-bonds formed between protein and drug molecule were analyzed through Gromacs utilities g_rmsd, g_rdf and g_hbond, respectively.

Results and Discussion

Virtual Screening and Molecular Docking Studies

It is believed that the compounds share the similar structure may have the similar function. Therefore, 95 % threshold similarity/cutoff was applied to screen the lead compounds. The result indicates that 92 compounds were identified similar to the currently active drug molecule, oseltamivir. Docking studies were performed to gain insight into the binding conformation of lead compounds derived from ligand-based VS techniques. The binding residues of the target structures were collected from the available literature evidences [34, 35]. In our earlier study, we have evaluated the binding site residues by means of available computer algorithms [55, 56]. Obviously, the evaluation and ranking of predicted ligand conformations are a crucial aspect of VS. In the present docking study, the binding affinity and the interactions found between ligands and the receptor were evaluated using scoring functions and reported in docking scores. The docking calculation is typically done for one ligand at a time and each calculation repeated twice to eliminate the false positive. In the docking analysis, a total of 92 compounds was then docked into active sites of native- and mutant-type NA crystal structures. The result is shown in Table 1. The docking score of native-type-oseltamivir complex was 4614 and H274Y–oseltamivir complex was 4602. This clearly indicates that mutation at the position H274Y in the NA structure significantly affect the binding of oseltamivir. As a result, docking score for H274Y–oseltamivir complex was significantly lesser than the native-type NA–oseltamivir complex. The docked complex is shown in Fig. 1. It is fact that, a potential lead compound should demonstrate higher scoring results than the currently active molecule. The 92 hits obtained from VS were also docked into the same site, producing 38 hits having higher dock score than oseltamivir when it binds with mutant-type NA. In which, 28 hits showed higher dock score with both native- and mutant-type structures. We have also noticed that 4 hits showed higher dock score with native-type rather than mutant-type of NA. Hence, we decided to further screen the 38 hits by means of bio-availability studies

Table 1 Docking score of the oseltamivir and lead compounds obtained from PubChem database against the target structure

S. No.	Compound ID	Score	
		2HTY	3CL0
1	Oseltamivir	4,614	4,602
2	**CID: 4603**	**4,510**	**4,656**
3	CID: 65028	4,524	4,456
4	CID: 24848267	4,482	4,566
5	CID: 25110712	4,530	4,536
6	CID: 25144224	4,530	4,536
7	**CID: 25145487**	**4,564**	**4,618**
8	CID: 25145488	4,530	4,536
9	CID: 25145489	4,530	4,536
10	CID: 25145490	4,460	4,420
11	**CID: 25145634**	**4,626**	**4,812**
12	CID: 40468108	4,696	4,476
13	**CID: 40468109**	**4,424**	**4,786**
14	CID: 40468110	4,384	4,484
15	**CID: 40468111**	**4,832**	**4,812**
16	**CID: 42052044**	**4,536**	**4,608**
17	**CID: 42052045**	**4,494**	**4,626**
18	**CID: 44512453**	**4,620**	**4,620**
19	**CID: 49849800**	**4,620**	**4,620**
20	CID: 49849802	4,368	4,512
21	CID: 51064085	4,544	4,418
22	CID: 51397619	3,432	3,418
23	**CID: 9928295**	**5,164**	**5,002**
24	**CID: 10713139**	**5,086**	**5,250**
25	CID: 46201075	3,432	3,418
26	**CID: 49849803**	**4,322**	**4,872**
27	CID: 11429373	4,556	4,380
28	CID: 11808666	4,216	4,278
29	CID: 20651751	4,160	4,540
30	CID: 21923401	4,368	4,492
31	CID: 40640966	4,266	4,480
32	CID: 40640968	4,304	4,370
33	CID: 40640970	4,238	4,352
34	CID: 40640972	4,080	4,356
35	CID: 44310478	4,188	4,306
36	CID: 51731106	4,746	4,426
37	**CID: 44514021**	**4,806**	**5,234**
38	**CID: 9967681**	**5,052**	**4,826**
39	**CID: 10546876**	**4,768**	**4,776**
40	**CID: 10640758**	**5,330**	**4,958**
41	**CID: 10784190**	**5,420**	**4,794**
42	**CID: 10784209**	**4,738**	**4,770**
43	CID: 24889058	3,650	3,610
44	**CID: 53423532**	**5,176**	**5,176**
45	**CID: 54498756**	**4,564**	**4,618**
46	**CID: 480262**	**4,654**	**4,928**

Table 1 continued

S. No.	Compound ID	Score	
		2HTY	3CL0
47	CID: 493854	4,708	4,346
48	**CID: 10763205**	**5,536**	**5,348**
49	**CID: 11441321**	**5,678**	**5,388**
50	**CID: 11961752**	**5,472**	**5,166**
51	**CID: 17753155**	**5,326**	**5,600**
52	CID: 22209881	4,870	4,426
53	**CID: 44514020**	**5,540**	**5,386**
54	**CID: 10881879**	**4,702**	**4,696**
55	CID: 20651763	4,388	4,160
56	**CID: 493855**	**5,200**	**4,630**
57	**CID: 6483690**	**5,200**	**4,630**
58	**CID: 10569862**	**5,124**	**5,030**
59	**CID: 10594009**	**5,328**	**4,654**
60	**CID: 10667491**	**5,036**	**5,002**
61	**CID: 10716405**	**4,372**	**4,676**
62	**CID: 11794953**	**5,552**	**5,132**
63	**CID: 11795748**	**5,408**	**5,144**
64	**CID: 22209882**	**4,932**	**4,750**
65	CID: 449381	4,132	4,452
66	CID: 480257	3,726	3,672
67	CID: 480258	4,204	3,928
68	CID: 480259	4,134	4,048
69	CID: 480261	3,956	4,318
70	CID: 480300	4,044	4,350
71	CID: 493852	4,572	4,166
72	CID: 493853	4,112	4,072
73	CID: 505923	4,162	3,854
74	CID: 4631786	4,234	4,504
75	CID: 6481597	4,148	4,468
76	CID: 6481598	4,234	4,504
77	CID: 6481599	3,728	3,948
78	CID: 6481600	4,204	3,928
79	CID: 15956756	3,920	4,264
80	CID: 20651701	4,286	3,848
81	CID: 20651739	4,306	4,364
82	CID: 20847166	4,162	4,354
83	CID: 22209879	4,520	4,194
84	CID: 22209880	4,508	4,514
85	CID: 25110713	4,106	4,556
86	CID: 40640967	4,032	4,190
87	CID: 40640969	4,126	4,386
88	CID: 40640971	4,462	4,322
89	**CID: 40640973**	**4,178**	**4,668**
90	**CID: 44345914**	**4,548**	**4,602**
91	CID: 44460822	4,140	4,158
92	CID: 49849804	4,110	4,154
93	CID: 49849805	4,110	4,154

Bold indicates the lead compounds showed higher binding score than oseltamivir

Bioavailability Analysis

The molecular properties and bioactivity for the lead compounds were predicted using Molinspiration program (www.molinspiration.com). The LogKow program [57] estimates the log octanol/water partition coefficient (logP) of organic chemicals and drugs by an atom/fragment contribution method developed at Syracuse Research Corporation [58]. Molecular polar surface area (TPSA) is calculated based on the methodology as a sum of fragment contributions. O- and N-centered polar fragments are considered. PSA has been shown to be a very good descriptor characterizing drug absorption, including intestinal absorption, bioavailability, $CaCo_2$ permeability, and blood–brain barrier penetration. log *P* value and PSA values are two important predictors of per oral bioavailability of drug molecules [59, 60]. Therefore, we calculated log *P* and PSA values along with other physiochemical properties such as molecular mass, the number of hydrogen bond acceptors, and the number of hydrogen bond donors for the all the 38 lead compounds obtained from the molecular docking study. The results showed that 36 molecules have zero violations of the rule of five which confirms that these molecules act as best drug molecules against NA (Table 2).

It is bare that for passing oral bioavailability criteria, number of rotatable bond should be <10 [44, 45]. Hence, further refinement of these hits was carried out by restricting the number of rotatable bonds to a maximum of ten. The number of rotatable bonds for all the 36 lead compounds was shown in Table 3. The result indicates that 18 compounds possess number of rotatable bonds <10. Therefore, it is expected that these compounds may exhibit good conformational flexibility than other lead compounds obtained in our study (Table 3).

Toxicity and Physicochemical Properties

Many drug candidates fail in the clinical trials, reasons are unrelated in the potency against the intended drug target. Pharmacokinetic and toxicity issues are blamed for more than half of all failure in the clinical trials. Therefore, it is essential to evaluate pharmacokinetic and toxicity of small molecules.

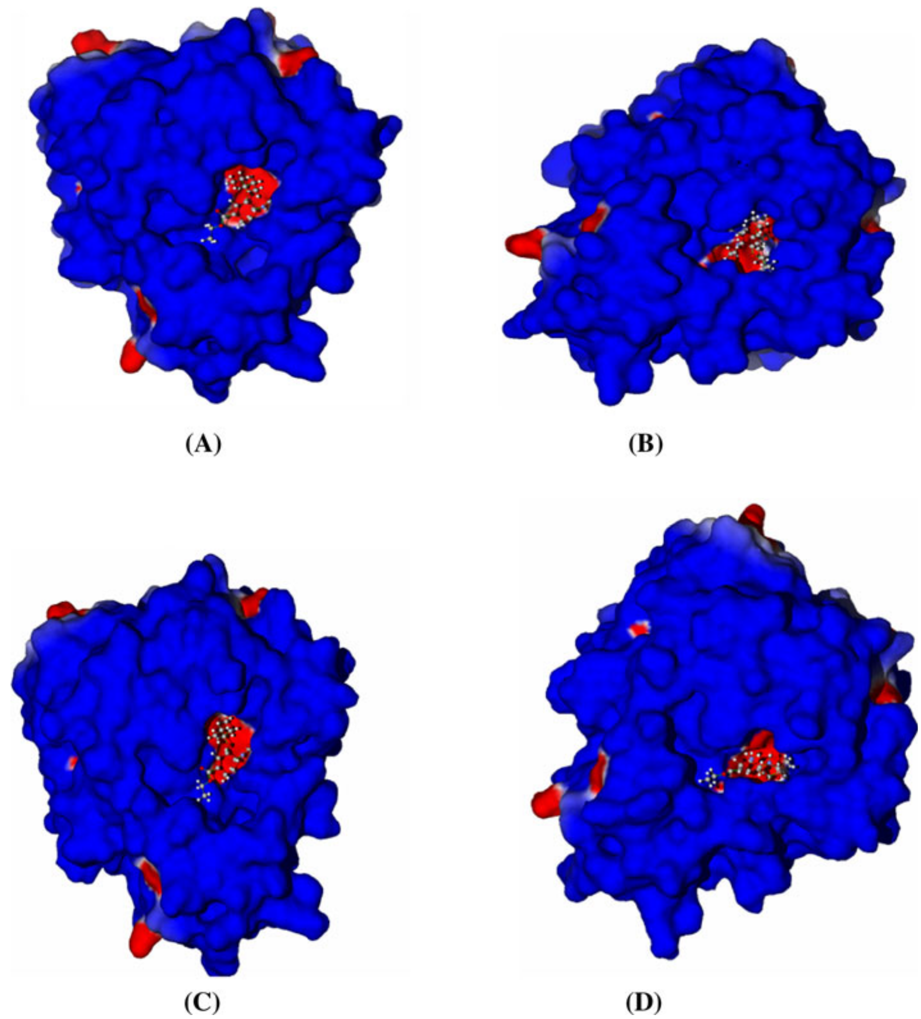

Fig. 1 Docked surface view of oseltamivir with native (**a**) and mutant (**b**) type of NA, virtual compound (CID 25145634) with native (**c**) and mutant (**d**) type of NA

The parameters, clogP and logS, were assessed to analyze the pharmacokinetic property of the filtered set of compounds. clogP is a well-established measure of the compound's hydrophilicity. Low hydrophilicities and therefore high log *P* values may cause poor absorption or permeation. It has been shown for compounds to have a reasonable probability of being well absorbed, their log *P* value must not be greater than 5.0. On this basis, all the 18 lead compounds are having log *P* values in the acceptable criteria.

Drug solubility is an important factor that affects the movement of a drug from the site of administration into the blood. It is known that insufficient solubility of drug can leads to poor absorption [41]. Our estimated log *S* value is a unit stripped logarithm (base ten) of a compound's solubility measured in mol/liter. There are more than 80 % of the drugs on the market have an (estimated) log *S* value greater than −4. Table 4 shows solubility of all the screened lead compounds. It is clear from the table that the solubility of the lead compounds was found in the comparable zone with that of standard drugs to fulfill the requirements of solubility and could be considered as a candidate drug for oral absorption.

Drug-Likeliness

The drug-likeliness is another important parameter. Because drug-like molecules exhibit favorable absorption, distribution, metabolism, excretion, toxicological (ADMET) parameters. Currently, there are many approaches to assess a compound drug-likeness based on topological descriptors, fingerprints of molecular drug-likeness structure keys or other properties such as clog *P* and MW [61]. In this study, Osiris program [47] was used for calculating the fragment-based drug-likeness of the lead compounds and comparing them with oseltamivir. It is interesting to note that CID 25145634 have significantly higher drug-likeness value (1.599), compared with oseltamivir (−1.499) and other lead compounds. This result indicates that CID 25145634 have distinct property in comparison with other lead molecules considered in our study.

Table 2 Calculations of molecular properties of oseltamivir and lead compound using molinspiration

S. No.	Lead compounds	miLogP	TPSA	MW	nON	nOHNH	nViolations	Volume
1	Oseltamivir	0.852	90.66	312.41	6	3	0	309.599
2	**CID 4603**	**0.852**	**90.66**	**312.41**	**6**	**3**	**0**	**309.599**
3	**CID 25145487**	**0.852**	**90.66**	**315.386**	**6**	**3**	**0**	**309.599**
4	**CID 25145634**	**0.852**	**90.66**	**317.37**	**5**	**3**	**0**	**197.381**
5	**CID 40468109**	**0.852**	**90.66**	**312.41**	**6**	**3**	**0**	**309.599**
6	**CID 40468111**	**0.852**	**90.66**	**312.41**	**6**	**3**	**0**	**309.599**
7	**CID 42052044**	**−1.353**	**92.279**	**313.418**	**6**	**4**	**0**	**310.398**
8	**CID 42052045**	**0.852**	**90.66**	**312.41**	**6**	**3**	**0**	**309.599**
9	**CID 44512453**	**0.852**	**90.66**	**312.41**	**6**	**3**	**0**	**309.599**
10	**CID 49849800**	**0.852**	**90.66**	**312.41**	**6**	**3**	**0**	**309.599**
11	**CID 9928295**	**0.852**	**90.66**	**312.41**	**6**	**3**	**0**	**309.599**
12	**CID 10713139**	**2.64**	**76.664**	**354.491**	**6**	**2**	**0**	**360.878**
13	**CID 49849803**	**0.852**	**90.66**	**312.41**	**6**	**3**	**0**	**309.599**
14	**CID 44514021**	**0.852**	**90.66**	**312.41**	**6**	**3**	**0**	**309.599**
15	**CID 9967681**	**2.678**	**114.392**	**338.408**	**8**	**1**	**0**	**323.202**
16	**CID 10546876**	**3.887**	**114.392**	**366.462**	**8**	**1**	**0**	**357.021**
17	**CID 10640758**	**2.877**	**114.392**	**338.408**	**8**	**1**	**0**	**323.417**
18	**CID 10784190**	**3.382**	**114.392**	**352.435**	**8**	**1**	**0**	**340.219**
19	**CID 10784209**	**2.406**	**76.664**	**352.475**	**6**	**2**	**0**	**355.246**
20	**CID 53423532**	**2.678**	**114.392**	**338.408**	**8**	**1**	**0**	**323.202**
21	**CID 57009670**	**2.605**	**76.664**	**352.475**	**6**	**2**	**0**	**355.461**
22	**CID 480262**	**0.978**	**101.654**	**312.41**	**6**	**4**	**0**	**308.873**
23	**CID 10763205**	**2.012**	**84.946**	**394.512**	**7**	**1**	**0**	**391.172**
24	**CID 11441321**	**4.595**	**102.969**	**412.527**	**8**	**2**	**0**	**404.868**
25	**CID 11961752**	**3.295**	**67.875**	**392.54**	**6**	**1**	**0**	**400.161**
26	**CID 17753155**	**4.279**	**102.969**	**396.484**	**8**	**2**	**0**	**383.214**
27	**CID 44514020**	**4.595**	**102.969**	**411.516**	**8**	**2**	**0**	**404.868**
28	**CID 10881879**	**2.302**	**114.392**	**324.381**	**8**	**1**	**0**	**306.4**
29	**CID 493855**	**1.574**	**101.654**	**326.437**	**4**	**6**	**0**	**325.89**
30	**CID 6483690**	**1.574**	**101.654**	**326.437**	**4**	**6**	**0**	**325.89**
31	**CID 10569862**	**2.715**	**114.392**	**350.419**	**8**	**1**	**0**	**334.373**
32	**CID 10594009**	**2.715**	**114.392**	**350.419**	**8**	**1**	**0**	**334.373**
33	**CID 10667491**	**4.392**	**114.392**	**380.489**	**8**	**1**	**0**	**373.823**
34	CID 10716405	5.403	114.392	408.543	8	1	1	407.426
35	**CID 11794953**	**4.898**	**114.392**	**394.516**	**8**	**1**	**0**	**390.624**
36	CID 11795748	5.258	114.392	408.543	8	1	1	407.211
37	**CID 22209882**	**1.574**	**101.654**	**412.246**	**6**	**4**	**0**	**325.89**
38	**CID 40640973**	**−0.14**	**101.654**	**284.356**	**6**	**4**	**0**	**275.27**
39	**CID 44345914**	**−0.14**	**101.654**	**284.356**	**6**	**4**	**0**	**275.27**

Bold indicates ADME screened compounds based on Lipinsiki rule of five

Toxicity

The toxicity risk predictor locates fragments within a molecule, which indicate a potential toxicity risk. Toxicity risk alerts are an indication that the drawn structure may be harmful concerning the risk category specified. From the data evaluated in Table 4 indicates that the 16 lead compounds were supposed to be non-mutagenic, non-irritating with no tumorigenic effects when run through the mutagenicity assessment system comparable with standard drugs used.

Drug Score

We have also examined the overall drug score (DS) for all the lead compounds and compared with that of standard

Table 3 Screening of compounds having good bioavailability

S. No.	Compound ID	nrotb
1	Oseltamivir	8
2	**CID 4603**	**8**
3	**CID 25145487**	**8**
4	**CID 25145634**	**8**
5	**CID 40468109**	**8**
6	**CID 40468111**	**8**
7	**CID 42052044**	**8**
8	**CID 42052045**	**8**
9	**CID 44512453**	**8**
10	**CID 49849800**	**8**
11	**CID 9928295**	**8**
12	CID 10713139	11
13	**CID 49849803**	**8**
14	**CID 44514021**	**8**
15	**CID 9967681**	**9**
16	CID 10546876	12
17	CID 10640758	10
18	CID 10784190	11
19	CID 10784209	11
20	CID 53423532	10
21	CID 57009670	12
22	**CID 480262**	**8**
23	CID 10763205	11
24	CID 11441321	11
25	CID 11961752	13
26	CID 17753155	12
27	CID 44514020	11
28	**CID 10881879**	**8**
29	CID 493855	10
30	CID 6483690	10
31	CID 10569862	10
32	CID 10594009	10
33	CID 10667491	13
34	CID 11794953	14
35	**CID 22209882**	**9**
36	**CID 40640973**	**6**
37	**CID 44345914**	**6**

Bold indicates lead compounds showed number of rotatable bonds <10

drugs oseltamivir. The drug score combines drug-likeliness, miLogP, log *S*, MW, and toxicity risks in one handy value than may be used to judge the compound's overall potential to qualify for a drug. The result is shown in Table 4.

The reported lead compounds showed moderate to good DS as compared with standard drug used. About nine compounds such as 25145487, 25145634, 40468109, 40468111, 44512453, 49849800, 9928295, 49849803, and 44514021 showed moderate to good drug score of more than 0.535. In particular, CID 25145634 showed very good drug score of 0.797 compared to the rest of the lead compounds in the analysis. The toxicity, drug-likeliness, and drug score results for the compound CID 25145634 are illustrated in Fig. 2. From the pharmacokinetic and pharmacodynamic analysis of all the lead compounds, we conclude that CID 25145634 showed better results in comparison with other lead compounds investigated in our study. The two-dimensional structure of oseltamivir was compared with CID 25145634 to get the structural characteristics. The result is shown in Fig. 3. It indicates that CID 25145634 are a deuterium-enriched oseltamivir. Furthermore, NMA approach was used to validate our conclusions.

Normal Mode Docking Studies

Gromacs package 4.5.3 was used to minimize the structure of native and mutant enzymes [30, 31]. One thousand steps of steepest descent energy minimization were carried out for the enzymes. The collective motion in the energy-minimized structure was generated by means of NMA [48]. It has been recently shown that half of the known protein movements can be modeled by using at most too low-frequency normal modes for explaining collective large amplitude motions of proteins in different conformational states [62]. These motions typically describe conformational changes which are essential for the functioning of proteins [63]. Hence, the lowest frequency mode (mode 7) [64] was used for our docking studies. The NMA generates 11 possible confirmations between DQMIN of −100 and DQMAX of 100 with DQSTEP step size of 20 for the target proteins specifying an amplitude range and increment in the NMA [49]. The 3D structure of oseltamivir and the lead compound (CID 25145634), deuterium-enriched oseltamivir, were generated by CORINA with the help of its SMILES string. It is to be noted that understanding the docking score between the target protein and the ligand molecule in all the 11 confirmations based on relevant normal modes will authorize the strength of docking process [65]. Hence, entire trajectory files from the lowest frequency mode were used as the input for docking analysis. The docking score for the oseltamivir and for the lead compound, CID 25145634, in all the 11 confirmations is shown in Table 5. We observed that docking score for CID 25145634 with native and mutant enzymes was substantially higher than oseltamivir in all the confirmations. This observation indicates that CID 25145634, deuterium-enriched oseltamivir, could bind more effectively to the native- and mutant-type NA than oseltamivir

Table 4 Toxicity risks and physicochemical properties of oseltamivir and virtual compounds predicted by OSIRIS property explorer

S. No.	Compound ID	Mutagenic	Tumorigenic	Irritant	cLogP	Solubility	Drug-likeness	Drug score
1	Oseltamivir	No	No	No	1.439	−2.448	−1.499	0.535
2	CID 4603	No	No	No	1.34	−2.712	−2.149	0.494
3	CID 25145487	No	No	No	3.164	−2.609	−0.886	0.548
4	**CID 25145634**	**No**	**No**	**No**	**1.804**	**−2.982**	**1.599**	**0.797**
5	CID 40468109	No	No	No	1.862	−2.628	−1.282	0.538
6	CID 40468111	No	No	No	1.862	−2.628	−1.282	0.538
7	CID 42052044	No	No	No	1.438	−2.448	−2.602	0.48
8	CID 42052045	No	No	No	2.81	−2.771	−2.359	0.47
9	CID 44512453	No	No	No	1.439	−2.448	−1.499	0.535
10	CID 49849800	No	No	No	0.992	−1.501	−1.753	0.553
11	CID 9928295	No	No	No	1.439	−2.448	−1.499	0.535
12	CID 49849803	No	No	No	1.439	−2.448	−1.499	0.535
13	CID 44514021	No	No	No	1.439	−2.448	−1.412	0.541
14	CID 9967681	No	No	Yes	3.787	−3.368	−6.092	0.229
15	CID 480262	No	No	No	1.478	−2.559	−2.261	0.394
16	CID 10881879	No	No	Yes	3.787	−3.368	−6.092	0.229
17	CID: 22209882	No	No	No	2.003	−2.722	−20.802	0.351

Bold indicates virtual compounds screened from toxicity test

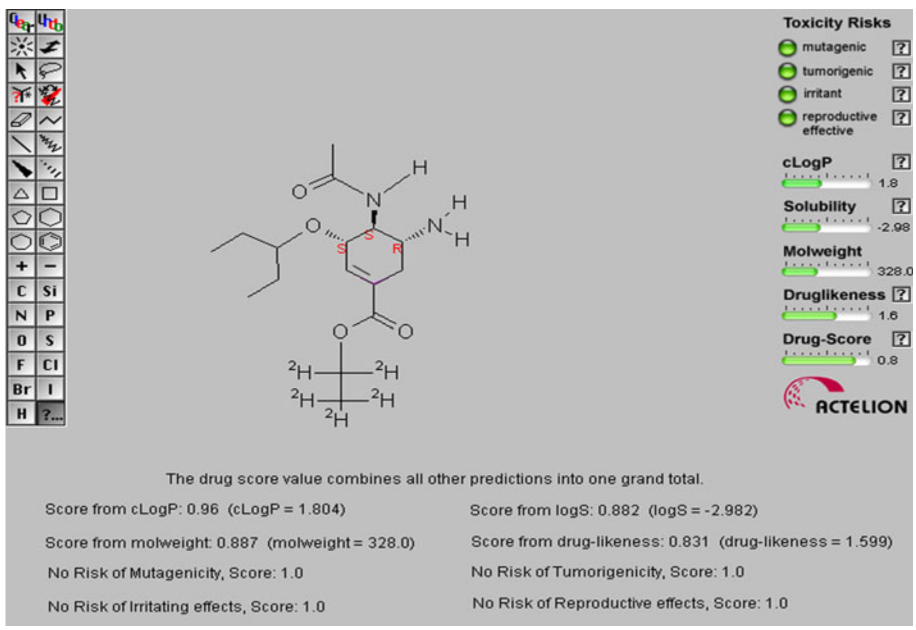

Fig. 2 Osiris property explorer showing drug-likeliness properties of CID 25145634

Molecular Dynamics Simulation

Molecular dynamic simulation was carried out by GROMACS [30, 31] which aimed to simulate the induced fit including potential conformational movements of both the protein and the ligand. Results showed that the average atom especially atoms of the NA–CID 25145634 complexes movements were small, fast convergence of energy, and charges in geometry (as measured by RMSD) were observed (Fig. 4). This highlights the stable binding of the lead compound, CID 25145634, with native- and mutant-type of NA. Figure 5a shows the radial distribution of oseltamivir with water oxygen atoms and Fig. 5b shows the radial distribution of CID 25145634 with water oxygen atoms. These results lead us to conclude that lead compound, CID 25145634, interacts well with water oxygen atoms in both native- and mutant-type of NA than oseltamivir. The intermolecular interactions between the NA with oseltamivir and CID 25145634 molecules were analyzed using *N*Hbond analysis. The analysis indicates that

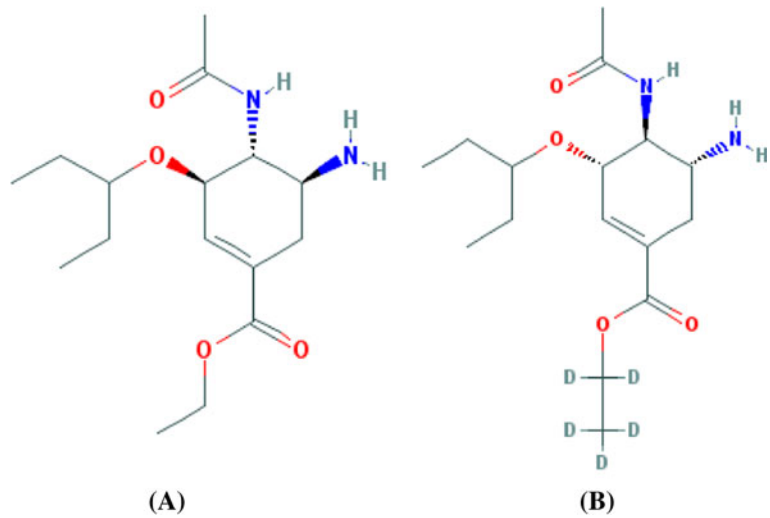

Fig. 3 Structure comparison between oseltamivir (**a**) and CID 25145634 (**b**)

Table 5 Normal mode docking analysis

Model	Frequency	Docking score of oseltamivir with the native type NA	Docking score of oseltamivir with the mutant type NA	Docking score of lead molecule with native type NA	Docking score of lead molecule with mutant type NA
1	−100	4,736	4,586	4,800	4,618
2	−80	4,614	4,432	4,694	4,698
3	−60	4,690	4,466	4,738	4,592
4	−40	4,678	4,388	4,690	4,534
5	−20	4,654	4,542	4,786	4,678
6	0	4,524	4,582	4,780	4,580
7	20	4,518	4,544	4,604	4,678
8	40	4,570	4,582	4,664	4,814
9	60	4,762	4,508	4,764	4,884
10	80	4,536	4,432	4,518	4,586
11	100	4,716	4,435	4,860	4,902

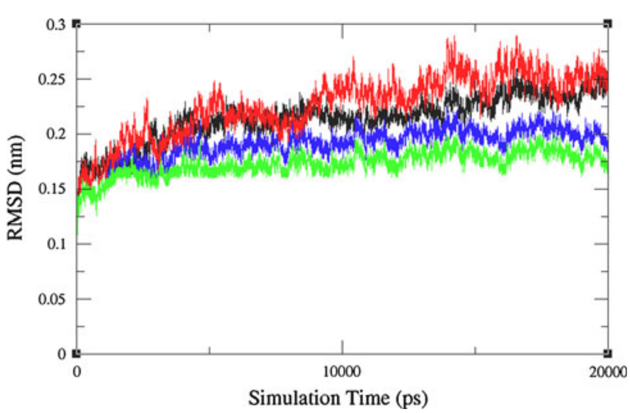

Fig. 4 Root mean square deviations correspond to native-type NA–oseltamivir complex (*black*), mutant-type NA–oseltamivir complex (*red*), native-type NA–CID 25145634 complex (*green*), and mutant-type NA–CID 25145634 complex (*blue*) along the MD simulation at 300 k (Color figure online)

native-type NA–oseltamivir complex was able to maintain eight intermolecular hydrogen bonds, whereas in the mutant-type NA–oseltamivir complex only four intermolecular hydrogen bonds were maintained throughout the simulation time (Fig. 6a). On the other hand, the lead compound, CID 25145634, able to maintain ten H-bonds throughout the simulation time (Fig. 6b) both with the native- and the mutant-type NA. This result indicates the prevalence of maximum number of intermolecular interaction in the NA–CID 25145634 complex. Therefore, we confirm that deuterium incorporated oseltamivir, CID 25145634, binds efficiently to NA than oseltamivir.

In conclusion, new drugs are desperately needed for the treatment drug-resistant H5N1 virus and innovative approaches are needed to identify new lead compounds that can enter the pipeline of lead optimization and therapeutic testing. In this study, we have used the computational approach to screen the lead molecule against H5N1 NA

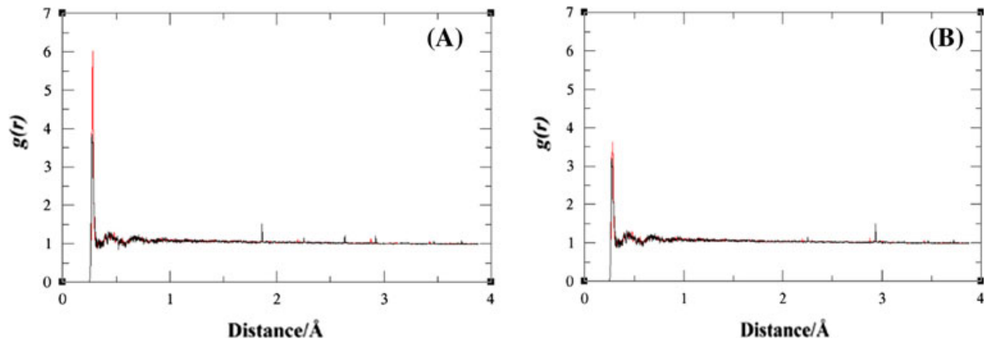

Fig. 5 **a** Radial distribution functions, g(r), centered on oseltamivir atoms to water oxygen atoms of the native-type NA–oseltamivir (*black*) and mutant-type NA–oseltamivir (*red*) complexes and **b** radial distribution functions, g(r), centered on CID 25145634 atoms to water oxygen atoms of the native-type NA–CID 25145634 (*black*) and mutant-type NA–CID 25145634 (*red*) complexes (Color figure online)

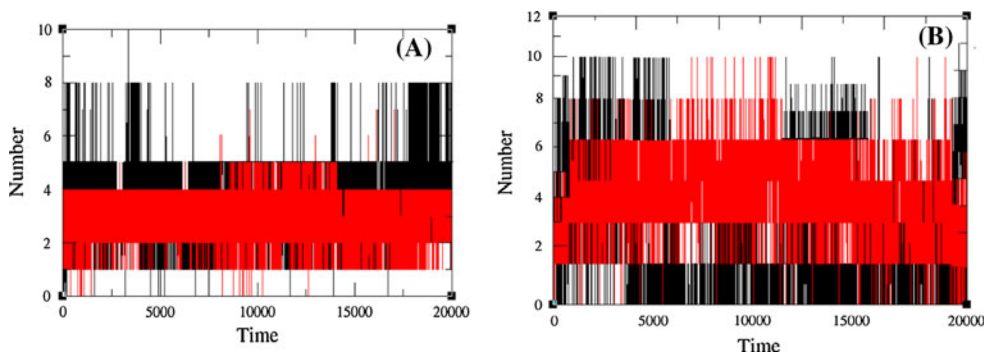

Fig. 6 **a** H Bonds observed between the native-type NA–oseltamivir complex (*black*) and mutant-type-NA oseltamivir complex (*red*). **b** Native-type NA–CID 25145634 complex (*black*) and mutant-type-NA CID 25145634 (*red*) complex during the MD simulation (Color figure online)

enzymes. Our approach demonstrated that CID 25145634 binds to influenza virus more tightly than oseltamivir. We have also predicted that CID 25145634 can bind to not only native-type but also resistant mutants of A/H5N1. The MOLINSPIRATION calculation undoubtedly indicates that CID 25145634 was found to express zero violations to the rule of five, hence an indication of favorable bio-availability based on drug-likeness. The considerable number of hydrogen donor/acceptor atoms incurred significant hydrophilic character into the drug. The structural comparison clearly indicates that CID 25145634 is a deuterium incorporated oseltamivir molecule. Deuterium (D or ^{2}H) is a naturally occurring, stable, non-radioactive isotope of hydrogen. It is believed that in favorable condition, the drug molecule with appropriate level of deuterium has the unique effect of retaining the biochemical potency and selectivity. The in silico toxicity profiles, drug-likeness, drug score, and molecular simulation data of CID 25145634 makes that this could be a promising leads for future development of safe and efficient antiviral agents. Finally, the results of RMSD, *N*Hbond, and radial distribution function data obtained from the molecular dynamics simulation studies undoubtedly indicates the stable binding CID 25145634 with native- and mutant-type of NA. The ingenuity and success of the computational approach discussed above bode well for the future prospects of finding new therapeutics which could results into massive reductions in therapeutics development time, which would provide us a hefty head-start against our antibiotic-resistant viral adversaries. Further investigation of this molecule using experimental approaches would be an interesting future direction.

Acknowledgments The authors express deep sense of gratitude to the management of Vellore Institute of Technology for all the support, assistance and constant encouragements to carry out this work. The authors also thank the reviewers for giving useful suggestions and comments in the improvement of this manuscript.

References

1. Mukhtar, M. M., Rasool, S. T., Song, D., Zhu, C., Hao, Q., Zhu, Y., et al. (2007). Origin of highly pathogenic H5N1 avian influenza virus in China and genetic characterization of donor and recipient viruses. *Journal of General Virology, 88*, 3094–3099.
2. Shirvan, A. N., Moradi, M., Aminian, M., & Madani, R. J. (2007). Preparation of neuraminidase-specific antiserum from the H9N2 subtype of avian influenza virus. *Turkish Journal of Veterinary and Animal Sciences, 31*, 219–223.
3. Matrosovich, M. N., Matrosovich, T. Y., Gray, T., Roberts, N. A., & Klenk, H. (2004). Neuraminidase is important for the initiation of influenza virus infection in human airway epithelium. *Journal of Virology, 78*, 12665–12667.
4. Su, Y., Yang, H. Y., Zhang, B. J., Jia, H. L., & Tien, P. (2008). Analysis of a point mutation in H5N1 avian influenza virus

hemagglutinin in relation to virus entry into live mammalian cells. *Archives of Virology, 153*, 2253–2261.
5. Takeda, M., Leser, G. P., Russell, C. J., & Lamb, R. A. (2003). Influenza virus hemagglutinin concentrates in lipid raft microdomains for efficient viral fusion. *Proceedings of the National Academy of Sciences, 100*, 14610–14617.
6. McKimm-Breschkin, J. L. (2000). Resistance of influenza viruses to neuraminidase inhibitors: A review. *Antiviral Research, 47*, 1–17.
7. Bauer, K., Richter, M., Wutzler, P., & Schmidtke, M. (2009). Different neuraminidase inhibitor susceptibilities of human H1N1, H1N2, and H3N2 influenza A viruses isolated in Germany from 2001 to 2005/06. *Antiviral Research, 82*, 34–41.
8. Matsuzaki, Y., Mizuta, K., Aoki, Y., Suto, A., Abiko, C., Sanjoh, K., et al. (2010). A two-year survey of the oseltamivir-resistant influenza A(H1N1) virus in Yamagata, Japan and the clinical effectiveness of oseltamivir and zanamivir. *Virology Journal, 7*, 53.
9. Ward, P., Small, I., Smith, J., Suter, P., & Dutkowski, R. (2005). Oseltamivir (Tamiflu) and its potential for use in the event of an influenza pandemic. *Journal of Antimicrobial Chemotherapy, 55*, i5–i21.
10. Mishin, V. P., Hayden, F. G., & Gubareva, L. V. (2005). Susceptibilities of antiviral-resistant influenza viruses to novel neuraminidase inhibitors. *Antimicrobial Agents and Chemotherapy, 49*, 4515–4520.
11. Le, Q. M., Kiso, M., Someya, K., Sakai, Y. T., Nguyen, T. H., Nguyen, K. H., et al. (2005). Avian flu: Isolation of drug-resistant H5N1 virus. *Nature, 437*, 1108.
12. de Jong, M. D., Tran, T. T., Truong, H. K., Vo, M. H., Smith, G. J., Nguyen, V. C., et al. (2005). Oseltamivir resistance during treatment of influenza A (H5N1) infection. *The New England Journal of Medicine, 353*, 2667–2672.
13. Gubareva, L. V., Kaiser, L., Matrosovich, M. N., Soo-Hoo, Y., & Hayden, F. G. (2001). Selection of influenza virus mutants in experimentally infected volunteers treated with oseltamivir. *The Journal of Infectious Diseases, 183*, 523–531.
14. Lackenby, A., Hungnes, O., Dudman, S. G., Meijer, A., Paget, W. J., Hay, A. J., et al. (2008). Emergence of resistance to oseltamivir among influenza A (H1N1) viruses in Europe. *Eurosurveillance, 13*, 8026.
15. Moscona, A. (2005). Oseltamivir resistance: Disabling our influenza defenses. *New England Journal of Medicine, 353*, 2633–2636.
16. Alves, I. D., Bechara, C., Walrant, A., Zaltsman, Y., Jiao, C. Y., & Sagan, S. (2011). Relationships between membrane binding, affinity and cell internalization efficacy of a cell-penetrating peptide: Penetratin as a case study. *PLoS One, 6*, e24096.
17. Monto, A. S. (2005). The threat of an avian influenza pandemic. *The New England Journal of Medicine, 352*, 323–325.
18. Monto, A. S. (2006). Vaccines and antiviral drugs in pandemic preparedness. *Emerging Infectious Disease, 12*, 55–60.
19. Oprea, T. I., & Matter, H. (2004). Integrating virtual screening in lead discovery. *Current Opinion in Chemical Biology, 8*, 349–358.
20. Chen, C. Y. C. (2008). Discovery of novel inhibitors for c-met by virtual screening and pharmacophore analysis. *Journal of the Chinese Institute of Chemical Engineers, 39*, 617–624.
21. Kitchen, D. B., Decornez, H., Furr, J. R., & Bajorath, J. (2004). Docking and scoring in virtual screening for drug discovery: Methods and applications. *Nature Reviews Drug Discovery, 3*, 935–949.
22. Wei, B. Q., Weaver, L. H., Ferrari, A. M., Matthews, B. W., & Shoichet, B. K. (2004). Testing a flexible-receptor docking algorithm in a model binding site. *Journal of Molecular Biology, 337*, 1161–1182.
23. Amaro, R. E., Baron, R., & McCammon, J. A. (2008). An improved relaxed complex scheme for receptor flexibility in computer-aided drug design. *Journal of Computer-Aided Molecular Design, 22*, 693–705.
24. Bowman, A. L., Nikolovska-Coleska, Z., Zhong, H., Wang, S., & Carlson, H. A. (2007). Small molecule inhibitors of the MDM2-p53 interaction discovered by ensemble-based receptor models. *Journal of the American Chemical Society, 129*, 12809–12814.
25. Bolton, E., Wang, Y., Thiessen, P. A., & Bryant, S. H. (2008). PubChem: Integrated platform of small molecules and biological activities. *Annual Reports in Computational Chemistry, 4*, 217–241.
26. Feldman, J., Snyder, K. A., Ticoll, A., Pintilie, G., & Hogue, C. W. (2006). A complete small molecule dataset from the protein data bank. *FEBS Letters, 580*, 1649–1653.
27. Xie, X. Q. (2010). Exploiting PubChem for virtual screening. *Expert Opinion on Drug Discovery, 5*, 1205–1220.
28. Berman, H. M., Westbrook, J., Feng, Z., Gilliland, G., Bhat, T. N., Weissig, H., et al. (2000). The protein data bank. *Nucleic Acids Research, 28*, 235–242.
29. Gasteiger, J., Rudolph, C., & Sadowski, J. (2009). Automatic generation of 3D-atomic coordinates for organic molecules. *Tetrahedron Computer Methodology, 3*, 537–547.
30. Hess, B., Kutzner, C., Spoel, D., & Lindahl, E. (2008). GROMACS 4: Algorithms for highly efficient, load-balanced, and scalable molecular simulation. *Journal of Chemical Theory and Computation, 4*, 435–447.
31. Spoel, D., Lindahl, E., Hess, B., Groenhof, G., Mark, A. E., & Berendsen, H. J. (2005). GROMACS: Fast, flexible, and free. *Journal of Computational Chemistry, 26*, 1701–1718.
32. Shoichet, B. K. (2004). Virtual screening of chemical libraries. *Nature, 432*, 862–865.
33. Tond, i. D., Slomczynska, U., Costi, M. P., Watterson, D. M., Ghelli, S., & Shoichet, B. K. (1999). Structure based discovery and in-parallel optimization of novel competitive inhibitors of thymidylate synthase. *Chemistry & Biology, 6*, 319–331.
34. Colman, P. M., Varghese, J. N., & Laver, W. G. (1983). Structure of the catalytic and antigenic sites in influenza virus neuraminidase. *Nature, 303*, 41–44.
35. Rungrotmongkol, T., Udommaneethanakit, T., Malaisree, M., Nunthaboot, N., Intharathep, P., Sompornpisut, P., et al. (2009). How does each substituent functional group of oseltamivir lose its activity against virulent H5N1 influenza mutants? *Biophysical Chemistry, 145*, 29–36.
36. Schneidman, D., Inbar, Y., Nussinov, R., & Wolfson, H. J. (2005). PatchDock and SymmDock: Servers for rigid and symmetric docking. *Nucleic Acids Research, 33*, 363–367.
37. Connolly, M. L. (1983). Solvent-accessible surfaces of proteins and nucleic acids. *Science, 221*, 709–713.
38. Connolly, M. L. (1983). Analytical molecular surface calculation. *Journal of Applied Crystallography, 16*, 548–558.
39. Zhang, C., Vasmatzis, G., Cornette, J. L., & DeLisi, C. (1997). Determination of atomic desolvation energies from the structures of crystallized proteins. *Journal of Molecular Biology, 267*, 707–726.
40. Ertl, P., Rohde, B., & Selzer, P. (2000). Fast calculation of molecular polar surface area as a sum of fragment based contributions and its application to the prediction of drug transport properties. *Journal of Medicinal Chemistry, 43*, 3714–3717.
41. Lipinski, C. A., Lombardo, F., Dominy, B. W., & Feeney, P. J. (1997). Experimental and computational approaches to estimate solubility and permeability in drug discovery and development settings. *Advanced Drug Delivery Reviews, 23*, 3–25.
42. Muegge, I. (2003). Selection criteria for drug-like compounds. *Medicinal Research Reviews, 23*, 302–321.

43. Buntrock, R. E. (2002). ChemOffice Ultra 7.0. *Journal of Chemical Information and Computer Sciences, 42*, 1505–1506.
44. Oprea, T. I. (2000). Property distribution of drug-related chemical databases. *Journal of Computer-Aided Molecular Design, 14*, 251.
45. Jeffery, G. H., Bassett, J., Mendham, J., & Denney, R. C. (1989). *Vogel's textbook of quantitative chemical analysis* (5th ed.). New York: Wiley.
46. Proudfoot, J. R. (2002). Drugs, leads, and drug-likeness: an analysis of some recently launched drugs. *Bioorganic & Medicinal Chemistry Letters, 12*, 1647–1650.
47. Sander, T. (2001). *OSIRIS property explorer*. Allschwil: Actelion Pharmaceuticals Ltd.
48. Tama, F., & Sanejouand, Y. H. (2001). Conformational change of proteins arising from normal mode calculations. *Protein Engineering, 14*, 1–6.
49. Suhre, K., & Sanejouand, Y. H. (2004). ElNemo: a normal mode web-server for protein movement analysis and the generation of templates for molecular replacement. *Nucleic Acids Research, 32*, 610–614.
50. Suhre, K., & Sanejouand, Y. H. (2004). On the potential of normal mode analysis for solving difficult molecular replacement problems. *Acta Crystallographica Section D, Biological Crystallography, 60*, 796–799.
51. Meagher, K. L., & Carlson, H. A. (2005). Solvation influences flap collapse in HIV-1 protease. *Proteins Structure, Function, and Bioinformatics, 58*, 119–125.
52. Schuttelkopf, A. W., & Van Aalten, D. M. F. (2004). PRODRG: A tool for high-throughput crystallography of protein–ligand complexes. *Acta Crystallogrphica, 60*, 1355–1363.
53. Darden, T., Perera, L., Li, L., & Pedersen, L. (1999). New tricks for modelers from the crystallography toolkit: The particle mesh Ewald algorithm and its use in nucleic acid simulations. *Structure, 7*, 55–60.
54. Lindahl, E., Hess, B., & van der Spoel, D. (2001). GROMACS 3.0: A package for molecular simulation and trajectory analysis. *Journal of Molecular Modeling, 7*, 306–317.
55. Karthick, V., Shanthi, V., Rajasekaran, R., & Ramanathan, K. (2012). Exploring the cause of oseltamivir resistance against mutant H274Y neuraminidase by molecular simulation approach. *Applied Biochemistry and Biotechnology, 16*, 237–249.
56. Karthick, V., Shanthi, V., Rajasekaran, R., & Ramanathan, K. (2012). In silico analysis of drug-resistant mutant of neuraminidase (N294S) against oseltamivir. *Protoplasma*. doi: 10.1007/s00709-012-0394-6.
57. Remko, M. (2009). Theoretical study of molecular structure, pKa, lipophilicity, solubility, absorption, and polar surface area of some hypoglycemic agents. *Journal of Molecular Structure: THEOCHEM, 897*, 73–82.
58. Wang, R., Fu, Y., & Lai, L. (1997). A new atom-additive method for calculating partition coefficients. *Journal of Chemical Information and Computer Sciences, 37*, 615–621.
59. Clark, D. E. (1999). Rapid calculation of polar molecular surface area and its application to the prediction of transport phenomena. *Journal of Pharmaceutical Sciences, 88*, 807–814.
60. Chang, L. C. W., Spanjersberg, R. F., von Frijtag Drabbe, K., unzel, J. K., Mulder-Krieger, T., van den Hout, G., et al. (2004). 2,4,6-Trisubstituted pyrimidines as a new class of selective adenosine A, receptor antagonists. *Journal of Medicinal Chemistry, 47*, 6529–6540.
61. Tetko, I. V. (2005). Computing chemistry on the web. *Drug Discovery Today, 10*, 1497–1500.
62. Delarue, M., & Dumas, P. (2004). On the use of low-frequency normal modes to enforce collective movements in refining macromolecular structural models. *Proceedings of the National Academy of Sciences of the United States of America, 101*, 6957–6962.
63. Alexandrov, V., Lehnert, U., Echols, N., Milburn, D., Engelman, D., & Gerstein, M. (2005). Normal modes for predicting protein motions: A comprehensive database assessment and associated Web tool. *Protein Science, 14*, 633–643.
64. Choudhury, D., Biswas, S., Roy, S., & Dattagupta, J. K. (2010). Improving thermostability of papain through structure-based protein engineering. *Protein Engineering, Design & Selection, 23*, 457–467.
65. Cavasotto, C. N., Kovacs, J. A., & Abagyan, R. A. (2005). Representing receptor flexibility in ligand docking through relevant normal modes. *Journal of the American Chemical Society, 127*, 9632–9640.